JOURNAL OF OPTOELECTRONICS AND ADVANCED MATERIALS Vol. 10, No. 4, April 2008, p. 907 - 912

Mg-based nanomaterials for energy storage

M. JURCZYK*, I. OKONSKA, M. NOWAK, M. JARZEBSKI
Institute of Materials Science and Engineering, Poznan University of Technology
M. Skłodowska-Curie 5 Sq., 60-965 Poznan, Poland

The paper present the advantages of some Mg-based nanostructured hydrogen storage materials. An amorphous and/or nanocrystalline Mg_2M (M=Fe, Ni, Cu) hydrogen storage alloys were prepared by mechanical alloying. For example, the powder 2Mg+Cu mixture mechanically alloyed for more than 18 h has transformed directly to an orthorhombic-type phase. In this powder, discharge capacity up to 26 mA h g^{-1} was measured. It was found that nickel substituting copper in $Mg_2Cu_{1-x}Ni_x$ alloy greatly improved the discharge capacity of studied material. In nanocrystalline Mg_2Ni powder, discharge capacities up to 100 mA h g^{-1} were measured. Additionally, it was found that the nickel powder addition to 2Mg+M/x wt% Ni is advantageous for the formation of Mg–M amorphous structure and for the improvement of the electrochemical properties of the studied alloys. On the other hand, the reaction of hydrogen gas with Mg_2M/Ni nanocomposite is enhanced significantly by the addition of catalysts such as titanium.

(Received February 25, 2008; accepted April 2, 2008)

Keywords: Mg-based nanomaterials, Mechanical alloying, Electrochemical properties, Hydrogen storage alloys

1. Introduction

The major problem in a future world with renewable energies and less environmental pollution is energy storage. Novel nanostructured materials may successfully solve this problem. Conventionally, the polycrystalline hydride materials have been prepared by arc or induction melting and annealing. However, either a low storage capacity by weight or poor absorption–desorption kinetics in addition to a complicated activation procedure have limited the practical use of metal hydrides [1]. Substantial improvements in the hydriding–dehydriding properties of metal hydrides could be possibly achieved by the formation of nanocrystalline structures by non-equilibrium processing technique such as mechanical alloying (MA) [2–7].

The amorphous or nanocrystalline metal hydrides offer a breakthrough in prospects for practical applications. Their excellent properties (significantly exceeding traditional hydrides) are a result of the combined engineering of many factors: alloy composition, surface properties, microstructure, grain size, and other [5]. In the development of metal hydrides, the goal is not only to improve operational properties of the existing hydrides, but also (more importantly) to create a new generation of materials, with the properties being designed and controlled to fulfil the particular demands of different applications.

A large number of experimental investigations on Mg-based compounds have been performed up to now in relation to their exceptional hydrogenation properties. Mg-based hydrogen storage alloys have been considered also to be possible candidates for electrodes in Ni-MH batteries [2, 3, 8, 9].

With current storage metallic materials it is not possible to exceed a capacity of 2 wt% H_2. Nevertheless for instance, magnesium can store 7 wt% H_2. Unfortunately MgH_2 is too stable and too much energy has to be expended in releasing the hydrogen. Alloying magnesium with other elements could lower the stability of the hydride without reducing the capacity to an unacceptable value. Mg_2Ni, one of the typical magnesium alloys, has great potential as a light hydrogen-storage alloy with high energy and is superior to the rare alloy of $LaNi_5$-type and to the alloy of ZrV_2-type with Laves phase in term of materials costs and the theoretical capacities. The theoretical capacity of the Mg_2Ni alloy is about three times capacity of $LaNi_5$ alloy. Mg_2 Ni alloy, however, can absorb and discharge hydrogen only at 200–300 °C and the speed of absorption and discharge is very slow. The electrochemical capacity of the polycrystalline Mg_2Ni alloy is too low to be a hydrogen-storage alloy.

It was found that the electrochemical activity of nanocrystalline hydrogen storage alloys can be improved in many ways, by alloying with other elements [5, 11], by ball-milling the alloy powders with a small amount of nickel or graphite powders [12–15]. For example, the surface modification of nanocrystalline hydrogen storage alloys with graphite by ball-milling leads to an improvement in both discharge capacity and charge-discharge cycle life [15, 16].

Recently, Xiao et al. have synthesized an amorphous 2Mg–Fe + x wt% Ni alloys by mechanical alloying [17]. The obtained result indicates that the nickel content does help to inhibit the corrosion of the alloy electrode in the KOH solution. On the other hand, the concentration of hydrogen in produced amorphous 2Mg+Fe/x wt% Ni alloys strongly decreases with increasing nickel contents [18].

As a continuation, of our previous works, in this paper, we have synthesized an amorphous and/or nanocrystalline Mg_2M (M=Fe, Ni, Cu) hydrogen storage alloys by mechanical alloying and 2Mg+M/x wt% Ni nanocomposites. The influence of microstructure on the structural, electrochemical and electronic properties on

synthesized materials was studied. These measurements may supply useful indirect information about the influence of the valence band structure, surface chemical composition, crystal structure, grain sizes, and preparation conditions on the hydrogenation properties of the studied materials.

2. Experimental details

Mechanical alloying was performed under an argon atmosphere using a SPEX 8000 Mixer Mill. The purity of the starting metallic elements Mg, Fe, Ni and Cu was 99.8, 99.5, 99.9% and 99.9%, respectively. The elemental powders (Mg: 44 μm; Fe: <10 μm; Ni: 3–7 μm; Cu: 3 μm) were mixed in the glove box (Labmaster 130) and poured into the vial. The mill was run up to 40 h for every powder preparation. The MA process of the 2Mg+M/Ni - type materials has been examined by X-ray diffraction (XRD) and microstructural investigations. The particle sizes were estimated by Scherrer method.

The Mg-based hydride syntheses were carried out in high-pressure reactor chamber of a conventional Sieverts-type volumetric system. The applied stainless steel reactor had the volume of 5 cm^3 and allowed for the performance of the pressure-composition (PC) isotherm measurements in the temperature range 18–625°C at H^2 gas pressure up to 10 MPa. The hydrogenation of the alloys was performed with the highest purity hydrogen gas obtained from $LaNi_5H_6$ hydrogen storage. The amount of absorbed hydrogen was determined from hydrogen pressure change in the reactor chamber. In order to secure an equilibrium state in the reactor, each sample was activated for 4 h in vacuum (4×10^{-4} Pa) at 400°C and the three hydrogenation–dehydrogenation cycles have been carried out before the PCT measurements were taken. The PC isotherms have been determined at temperature 300°C in the dehydrogenation process. The H_2 pressure in the reactor chamber was determined with an accuracy of $\pm 1 \times 10^{-4}$ MPa, whereas the temperature was kept constant with the accuracy of ±0.2°C. Allowance for the coefficient of hydrogen compressibility made it possible to calculate the hydrogen concentration in the sample with an accuracy of ± 0.02 H atoms per f.u.

The mechanically alloyed (amorphous) and annealed (nanocrystalline) materials with 10 wt% addition of Ni powder, were subjected to electrochemical measurements as working electrodes after pressing (under 80 kN cm^{-2}) to 0.5 g pellet form between nickel nets acting as current collector. The diameter of each electrode was 10.4 mm and the thickness of approximately 1.4 mm. Soaking of the electrodes in 0.01M NH_4F solution for 1 h at room temperature was sufficient for the initial activation. The constant current charge/discharge measurements were performed at current density of i = 4 mA g^{-1}. The electrochemical properties of electrodes were measured in a three-compartment glass cell, using a much larger $NiOOH/Ni(OH)_2$ counter electrode and a Hg/HgO/6 M KOH reference electrode. All electrochemical measurements were carried out in deaerated 6 M KOH solution prepared from Analar grade KOH and 18 $M\Omega cm^{-1}$ water, at 20°C. Potentiodynamic and galvanostatic techniques with either short or long-term pulses using a conventional apparatus were applied to study the charge-discharge kinetics of the electrodes. A detailed description of the electrochemical measurements was given in [8].

3. Results and discussion

The behaviour of MA process has been studied by X-ray diffraction and microstructural investigations. In this work, we have synthesized an amorphous and/or nanocrystalline Mg_2M (M=Fe, Ni, Cu) hydrogen storage alloys by mechanical alloying and 2Mg+M/x wt% Ni nanocomposites.

3.1. Mg_2Cu - type alloys

Fig. 1 shows a series of XRD spectra of mechanically alloyed 2Mg-Cu powder mixture (0.433 wt% Mg + 0.567 wt% Cu) subjected to milling in increasing time. During mechanical alloying the originally sharp diffraction lines of Mg and Cu gradually become broader and their intensities decrease with milling time (Fig. 1b). The powder mixture milled for more than 18 h has transformed directly to an orthorhombic-type phase. Finally, the obtained powder was heat treated in high purity argon atmosphere at 450°C for 0.5 h to obtain the desired microstructure. All diffraction peaks were assigned to those of orthorhombic-type structure with cell parameters a = 9.119(4) Å, b = 18.343(4) Å, c = 5.271(1) Å (Fig. 1d).

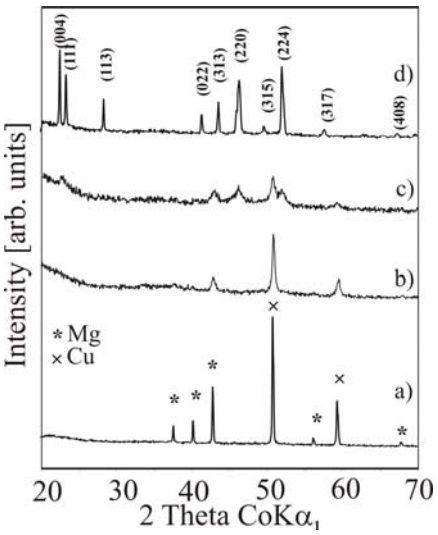

Fig. 1. XRD spectra of a mixture of 2Mg and Cu powders mechanically alloyed for different times in an argon atmosphere: initial state (elemental powder mixture) (a), after MA for 4.5 h (b), after MA for 18 h (c) and heat treated at 450°C for 0.5 h (d)

Table 1 reports the cell parameters of all the studied materials. According to the Scherrer method for XRD profiles, the average size of 2Mg-Cu mechanically alloyed for 40 h powders was of the order of 30 nm; after heat

treatment in high purity argon atmosphere at 450°C for 0.5 h the mean crystallite size of the nanocrystalline alloy estimated from AFM experiment was about 50 nm.

Table 1. Structure, lattice parameters and discharge capacities for studied nanocrystalline, microcrystalline and amorphous Mg-based materials.

Material	Structure and lattice constants (Å)	Discharge capacity (mA h/g)	
		1st cycle	10th cycle
nanocrystalline Mg_2Cu	orthorhombic a = 9.119 b = 18.343 c = 5.271	26.5	–
microcrystalline Mg_2Cu	orthorhombic a = 9.066 b = 18.360 c = 5.283	25.2	–
amorphous 2Mg+Cu/100 wt% Ni	–	132	82
nanocrystalline Mg_2Ni	hexagonal a=5.216 c=13.246	100	5
microcrystalline Mg_2Ni	hexagonal a=5.223 c=13.30	–	–
amorphous 2Mg+Ni/100 wt% Ni	–	175	90
amorphous 2Mg+Fe/0 wt% Ni	–	0	0
amorphous 2Mg+Fe/100 wt% Ni	–	155	45
amorphous 2Mg+Fe/200 wt% Ni	–	134	75

At room temperature, the original nanocrystalline Mg_2Cu alloy absorbs hydrogen, but almost does not desorb it. At temperatures above 250°C the kinetic of the absorption-desorption process improves considerably and for nanocrystalline Mg_2Cu alloy the reaction with hydrogen is reversible. Upon hydrogenation, Mg_2Cu transforms into the hydride MgH_2+$MgCu_2$ phases. At at 300°C the maximum absorption capacity reaches 2.25 wt% for pure nanocrystalline Mg_2Cu alloy. This is lower than in the microcrystalline Mg_2Cu alloy (2.6 wt%) because of a significant amount of strain, chemical disorder and defects introduced into the material during the mechanical alloying process [19].

The Mg_2Cu electrode, mechanically alloyed and annealed, displayed the maximum discharge capacity (26.5 mA h g^{-1}) at the 1st cycle but degraded strongly with cycling (see Table 1). The poor cyclic behaviour of Mg_2Cu electrodes is attributed to the formation of $Mg(OH)_2$ on the electrodes, which has been considered to arise from the charge-discharge cycles [8].

3.2 Mg_2Ni - type alloys

Fig. 2 shows a series of XRD spectra of mechanically alloyed 2Mg-Ni powder mixture (0.453 wt % Mg + 0.547 wt % Ni) subjected to milling in increasing time. The originally sharp diffraction lines of Mg and Ni (Fig. 2a) gradually become broader and their intensity decreases with milling time. The nanostructured Mg_2Ni with broad diffraction peaks are already found after 5 h of MA process. The powder mixture milled for more than 30 h has transformed directly to a hexagonal-type phase (Fig. 2b). Finally, the obtained powder was heat treated in high purity argon atmosphere at 450°C for 0.5 h to obtain the desired microstructure (Fig. 2c). All diffraction peaks were assigned to those of the hexagonal crystal structure with cell parameters a=5.216 Å, c=13.246 Å. Table 1 reports the cell parameters of all the studied materials. The average size of amorphous 2Mg-Ni powders, according to AFM studies, was of the order of 30 nm.

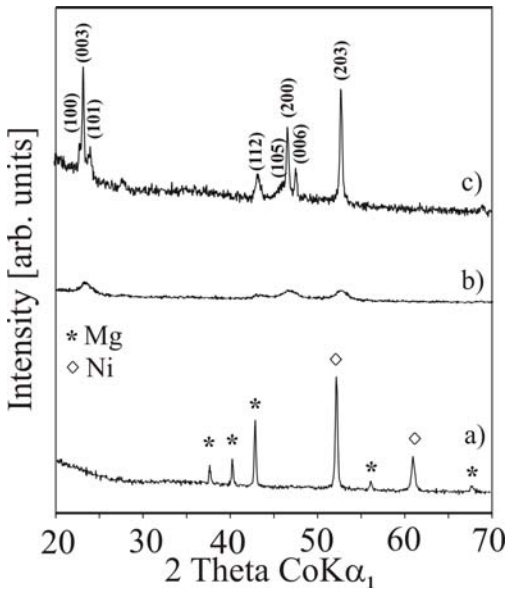

Fig. 2. XRD spectra of a mixture of 2Mg and Ni powders: initial state (elemental powder mixture (a)), after MA for 30 h (b) and heat treated at 450oC for 0.5 h (c).

At room temperature, the original nanocrystalline alloy, Mg_2Ni, absorbs hydrogen, but almost does not desorb it. At temperatures above 250 °C the kinetic of the absorption-desorption process improves considerably and for nanocrystalline Mg_2Ni alloy the reaction with hydrogen is reversible. The hydrogen content in this material at 300°C is 3.25 wt%. Upon hydrogenation, Mg_2Ni transforms into the hydride Mg_2Ni-H phase. It is important to note, that between 245-210°C the hydride Mg_2Ni-H phase transforms from a high temperature cubic structure to a low temperature monoclinic phase [20]. When hydrogen is absorbed by Mg_2Ni beyond 0.3 H per formula unit, the system undergoes a structural rearrangement to the stoichiometric complex Mg_2Ni-H hydride, with an accompanying 32% increase in volume.

The Mg_2Ni electrode, mechanically alloyed and annealed, displayed the maximum discharge capacity (100 mA h g^{-1}) at the 1st cycle but degraded strongly with cycling. The poor cyclic behaviour of Mg_2Ni electrodes is attributed to the formation of $Mg(OH)_2$ on the electrodes, which has been considered to arise from the charge-discharge cycles [21].

On the other hand, the surface chemical composition of nanocrystalline Mg_2Ni-type alloy studied by X-ray photoelectron spectroscopy (XPS) showed the strong surface segregation under UHV conditions of Mg atoms in the MA nanocrystalline Mg_2Ni alloy. This phenomenon could considerably influence the hydrogenation process in such a type of materials, too. The same surface segregation was observed earlier by Stefanov in Mg-Ni films, where magnesium was found to segregate at the surface [22].

3.3. 2Mg+Fe/x wt% Ni - type material

Mg and Fe do not form an intermetallic compound; this results in difficulties in the preparation of its hydride phase. Recently, the direct synthesis of Mg_2FeH_6 by mechanical alloying in hydrogen atmosphere has been investigated [18]. The structure of Mg_2FeH_6 is cubic of K_2PtC_{l6} type. Fig. 3 shows a series of XRD spectra of mechanically alloyed 2Mg+Fe/x wt% Ni powder mixtures for 48 h. It can be seen that only Mg and α-Fe lines are observed for nickel-free 2Mg+Fe powder mixture (Fig. 3a). The nickel addition is advantageous for the formation of amorphous structures (Fig. 3 b,c). But differentiation between a "truly" amorphous, extremely fine grained or a material in which very small crystals are embedded in an amorphous matrix in so produced materials has not been easy on the basis of diffraction basis. According to the Scherrer method for XRD profiles, the average size of 2Mg+Fe mechanically alloyed for 48 h powders was of the order of 30 and 42 nm for Mg and α-Fe, respectively (Table 1). On the other hand, for 2Mg+Fe/x wt% Ni powder mixtures MA for 48 h the average particle sizes were 29 and 18 nm for x=100 and 200 wt% of Ni, respectively. Xiao at al. pointed that the ball-milled (2Mg+Fe/200 wt% Ni) may be amorphous 2Mg–Fe alloy which are inlaid with microcrystalline/nanocrystalline Ni particles homogeneously [17].

Recently, we have studied the microstructure and possible local ordering in the mechanically alloyed TiNi samples by TEM [23]. The sample milled for 5 h was mostly amorphous as appears from a high resolution image. SAED pattern contains broad rings at positions expected for TiNi with CsCl structure. There are, however additional weak, diffuse rings, most probably from TiO_2. It has been found that the amorphous alloy was unstable upon exposure to electron beam and underwent some crystallization. Apart from prevailing amorphous phase, the milled sample contained small amount of crystalline alloy with CsCl structure. Lack of any sharp reflections in the XRD pattern suggests that the amount of the crystalline phase is very low and/or it forms during in TEM observation.

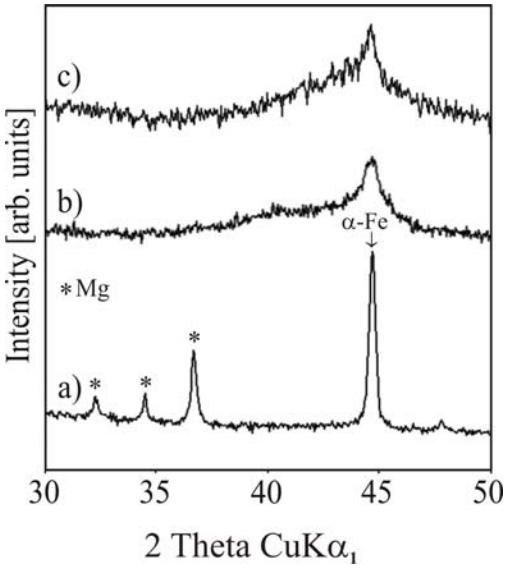

Fig. 3. XRD spectra of a nanoscale 2Mg+Fe/x wt% Ni materials: x=0 (a), x=100 (b) and x=200 (c).

At room temperature, the mechanically alloyed 2Mg+Fe alloy absorbs hydrogen, but almost does not desorb it. At temperatures above 250°C the kinetics of the absorption–desorption process improves considerably and for 2Mg+Fe mixture the reaction with hydrogen is reversible. Upon hydrogenation, 2Mg+Fe mixture transforms into the MgH_2 + α-Fe phases. A similar phenomenon to that described here has been observed earlier by us in nanostructured Mg_2Cu alloy [9]. On the other hand, upon hydrogenation, 2Mg+Fe/100 wt% Ni and 2Mg+Fe/200 wt% Ni mixtures transform into the Mg_2FeH_6 + α-Fe + Ni and α-Fe + Ni, respectively. The maximum absorption capacity reaches 3.25 wt% for 2Mg+Fe mixture. This is higher than in the nanocrystalline Mg_2Cu alloy (2.25 wt%).The concentration of hydrogen in produced amorphous 2Mg+Fe/x wt% Ni materials strongly decreases with increasing nickel contents (Table 1).

The cycling dischargeability of 2Mg+Fe/x wt% Ni electrode alloys is shown in Fig. 4. The 2Mg+Fe electrode, mechanically alloyed, displayed the zero discharge capacity. The discharge capacity of amorphous 2Mg+Fe high energy ball milled with Ni was improved. With increasing nickel content in the studied Mg-Fe materials, at first cycle, the discharge capacity increases first and then decreases, and for x = 100 reaches a maximum value of 155 mAh g^{-1}. For 2Mg+Fe/200 wt% Ni, after 10 cycles, the discharge capacity is higher than 70 mAh g^{-1}. The elemental nickel was distributed inside of mechanically alloyed Mg-Fe particles homogenously. It is generally agreed that the role of nickel particles is to catalyze the electrochemical reaction and/or reduce the diffusion resistance of hydrogen. High energy ball milling of 2Mg+Fe with nickel effectively reduced the degradation rate of the studied electrode material. The higher the Ni content is, the more resistant the alloy is to the corrosion of the alkaline electrolyte.

Generally, the poor cyclic behaviour of 2Mg+Fe/Ni electrodes is attributed to the formation of $Mg(OH)_2$ on the

electrodes, which has been considered to arise from the charge-discharge cycles [21]. Generally, the amorphous structure is easily formed with increasing Ni content in the alloys, and the amorphous alloys have good corrosion resistance property. This fact can improve the cycling stability of the alloys.

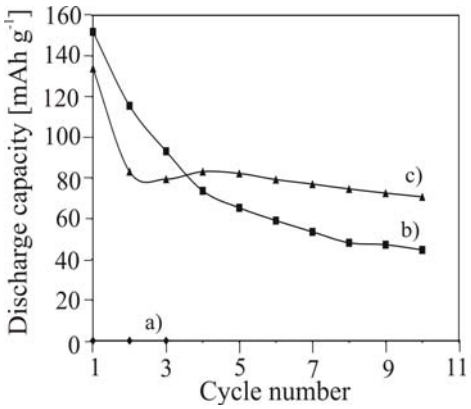

Fig. 4. Discharge capacities of amorphous 2Mg+Fe/x wt% Ni: x = 0 (a), x = 100 (b) and x = 200 (c); (current density of charge/discharge was 4 mA g^{-1}).

Application of Mg-based alloys focused our attention also on the electronic structure of hydrogen storage materials [7, 10]. Similarly to the effect of the band broadening observed for the nanocrystalline TiFe and $LaNi_5$ based alloys, we have observed such a modification in the case of the Mg-based system. Especially, a clear broadening of the band can be visible when compared experimental and theoretical XPS valence band for the Mg_2Ni or Mg_2Cu systems. The observed strong modifications of the electronic structure of the nanocrystalline Mg-based hydrogen storage materials significantly influenced their hydrogenation properties. The reasons responsible for the band broadening in the amorphous 2Mg+Fe/x wt% Ni and nanocrystalline Mg_2Ni and Mg_2Cu alloys are probably associated with a strong deformation of the nanocrystals in the MA samples [24]. Normally the interior of the nanocrystal is constrained and the distances between atoms located at the grain boundaries expanded. The valence band spectra of the MA samples could be also broadened due to an additional disorder introduced during formation of the nanoscale structure.

Independently, the effect of Ni content on the electrochemical and surface characteristics of Mg-Ti-Ni ternary hydrogen storage electrode alloys has been studied, as well. The cycling discharge degradation rate gradually decreases with the increase nickel content. XPS analysis reveals that the outmost surface layer on the Mg-Ti-Ni alloys is a $Mg(OH)_2$ passive film, in which the content of Mg increases, and the degree of oxidation of Mg becomes higher as the cycling goes on. Below the $Mg(OH)_2$ film is a composite layer of several oxides including NiO, TiO_2 and $Mg(OH)_2$. This layer is insoluble and compact, and helps to inhibit further corrosion of the fresh alloy surface underneath.

4. Conclusion

Nanocrystalline Mg_2M-type alloys (M=Cu, Ni) were synthesized by mechanical alloying and annealing. It was found that the respective replacement of Cu by Ni in $Mg_2Cu_{1-x}Ni_x$ alloy leads to an increase in discharge capacity, at room temperature. Additionally, it was found that milling of 10 wt% of nickel is sufficient to improve the discharge capacity of studied Mg-based nanocomposites. On the other hand, the nickel addition in amorphous 2Mg+Fe/x wt% Ni alloys is advantageous for the formation of Mg–Fe amorphous structures and for the improvement of the electrochemical properties of the studied alloys.

The experimental XPS valence bands measured for MA nanocrystalline alloys showed a significant broadening compared to those obtained for the microcrystalline samples with the same chemical composition. This is probably due to a strong deformation of the nanocrystals in the mechanically alloyed samples.

Acknowledgements

The financial support of the Polish Ministry of Education and Science under the contract PBZ-KBN-117/T08/07 is gratefully acknowledged.

References

[1] see for example: Nanoscale materials for energy storage, all articles in: Mater. Sci. Eng. B. **108**, 1 (2004).
[2] A. Anani, A. Visintin, K. Petrov, S. Srinivasan, J. J. Reilly, J. R. Johnson, R. B. Schwarz, P. B. Desch, J. Power Sources **47**, 261 (1994).
[3] L. Zaluski A. Zaluska, J. O. Ström-Olsen, J. Alloys Comp. **253-254**, 70 (1997).
[4] L. Schlapbach, A. Züttel, Nature (London) **414**, 353 (2001).
[5] M. Jurczyk, Bull. Pol. Ac.: Tech. **52**, 67 (2004).
[6] S. Orimo, A. Züttel, K. Ikeda, S. Saruki, T. Fukunaga, H. Fujii, L. Schlapbach, J. Alloys Comp. **293-295,** 437 (1999).
[7] M. Jurczyk, L. Smardz, A. Szajek, Mat. Sc. Eng., B **108**, 67 (2004).
[8] A. Gasiorowski, W. Iwasieczko, D. Skoryna, H. Drulis, M. Jurczyk, J. Alloys Comp. **364**, 283 (2004).
[9] M. Jurczyk, I. Okonska, W. Iwasieczko, E. Jankowska, H. Drulis, J. Alloys Comp. **429**, 316 (2007).
[10] A. Szajek, M. Jurczyk, I. Okonska, K. Smardz, E. Jankowska, L. Smardz, J. Alloys Comp. **436**, 345 (2007)
[11] S. I. Orimo, H. Fujii, Intermetallics **6**, 185 (1998).
[12] M. Au, F. Pourarian, S. Simizu, S. G. Sankar, L. Zhang, J. Alloys Comp. **223**, 1 (1995).
[13] D. Sun, M. Latroche, A. Percheron-Guégan, J. Alloys Comp. **257**, 302 (1997).
[14] S. Nohara, H. Inoue, Y. Fukumoto, C. Iwakura,

J. Alloys Comp. **252**, L16 (1997).
[15] S. Bouaricha, J.P. Dodelet, D. Guay, J. Huot, R. Schultz, J. Alloys Comp. **325**, 245 (2001).
[16] M. Jurczyk, J. Mater. Sc. **39**, 5271 (2004).
[17] Xiao Xuezhang, Wang Xinhua, Gao Linhui, Wang Li, Chen Changpin, J. Alloys Comp. **413**, 312 (2006).
[18] I. Okonska, W. Iwasieczko, M. Jarzebski, M. Nowak, M. Jurczyk, Int. J. Hydrogen Energy (2007), in print.
[19]C. Suryanarayana, Progr. Mater. Science **46**, 1 (2001)
[20] M. Gupta, E. Berlin, L. Schalpbach, J. Less-Common Met. **103**, 389 (1984).
[21] D. Mu, Y. Hatano, T. Abe, K. Watanabe, J. Alloys Comp. **334**, 232 (2002).
[22] P. Stefanov, Vacuum **47**, 1107 (1996).
[23] M. Jurczyk, M. Nowak, Nanostructured Materials in Electrochemistry, Wiley-VCH, Chapter 9, (Ed.) Eftekhari, (2007), in press.
[24] L. Smardz, K. Smardz, M. Nowak, M. Jurczyk, Cryst. Res. & Techn. **36**, 1385 (2001).

*Corresponding author: Jurczyk@sol.put.poznan.pl